AIMS Mathematics, 10(11): 27016–27043.
DOI: 10.3934/math.20251187
Received: 06 September 2025
Revised: 28 October 2025
Accepted: 13 November 2025
Published: 21 November 2025

https://www.aimspress.com/journal/Math

Research article

A new log-adjusted polynomial Fréchet model for heavy-tailed PORT-VaR analysis and one-step-ahead-VaR forecasting in finance and economics

Abdussalam Aljadani*

Department of Management, College of Business Administration in Yanbu, Taibah University, Yanbu Governorate, Saudi Arabia

* **Correspondence:** Email: ajadani@taibahu.edu.sa, abdussalamamaljadani@gmail.com.

Abstract: This paper introduced a new statistical model for analyzing extreme risks in economic and financial contexts called the log-adjusted polynomial Fréchet (LAPFr) distribution. The proposed distribution offers enhanced flexibility in capturing heavy-tailed behavior, a hallmark of real insurance and financial datasets. Here, the model was applied to two empirically relevant datasets: Boston housing prices and U.S. reinsurance financial revenues, focusing on tail risk estimation and one-step-ahead value-at-risk (VaR) forecasting. Key actuarial risk measures, including VaR, expected shortfall (ExSh), tail variance (TV), tail mean variance (TMV), mean of order P (MOOP), and peaks over random threshold (PORT-VaR), are computed and analyzed across multiple confidence levels. A risk-adjusted return on capital (RAROC) assessment further illustrates the trade-off between return and tail risk, offering practical insights for risk managers and insurers. The number of exceedances above VaR thresholds was examined both numerically and graphically, revealing patterns in the frequency and severity of extreme events. Finally, the one-step-ahead VaR forecast in finance and economics were presented as a part of the risk analysis process.

Keywords: actuarial risk; economic data; finance data; peaks over a random threshold value-at-risk; risk analysis; risk-adjusted return on capital; value-at-risk
Mathematics Subject Classification: 60E05; 62E10; 62H05; 62P05; 62F10; 62F15

1. Introduction

In recent years, the increasing volatility in financial and insurance markets has highlighted the limitations of conventional risk models in capturing extreme events. Traditional approaches often fail to adequately describe the heavy-tailed nature of losses, leading to severe underestimation of tail risk. This is particularly evident in sectors like real estate and reinsurance, where rare but large shocks can have systemic consequences. The Fréchet distribution, known for its ability to model heavy tails, provides a useful foundation but lacks sufficient flexibility in shaping tail behavior.

To address this research gap, we incorporate the Fréchet (Fr for short) model into the log-adjusted polynomial (LAP) family (see [1]), creating a more adaptable and realistic model. The resulting LAPFr distribution enhances tail modeling by introducing additional shape parameters through a weighted exponential structure. It allows for better fit and more accurate risk assessment in the upper tail, where extreme values reside. Our focus extends beyond mere fitting: we aim to improve practical risk measures such as VaR, ExSh, and RAROC under extreme conditions. Furthermore, we employ the PORT-VaR and MOO$^{\mathrm{P}}$ methodologies to analyze peaks over random thresholds, offering deeper insight into exceedance patterns. This work bridges theoretical development with real application, providing a robust tool for actuaries, financial analysts, and risk managers dealing with extreme events. According to [2], the LAP family is defined by the following cumulative distribution function (CDF):

$$F\left(x;\beta,\underline{\Phi}\right) = C\ log\left[1 + G\left(x;\underline{\Phi}\right)\right] e^{\beta G\left(x;\underline{\Phi}\right)}, \quad x \in R, \tag{1}$$

where $\beta > 0$ is a shape parameter,

$$C = \frac{1}{e^{\beta}\ log(2)},$$

and $G\left(x;\underline{\Phi}\right)$ is a baseline CDF with the corresponding probability density function (PDF) $g\left(x;\underline{\Phi}\right)$ which depends on the parameter $\underline{\Phi}$. The CDF of the Fr distribution is given by (for $x > 0$):

$$G(x;\alpha,\theta) = exp\left[-\left(\frac{\alpha}{x}\right)^{\theta}\right], \tag{2}$$

where $\alpha > 0$ is a scale parameter and $\theta > 0$ is a shape parameter. From an economic standpoint, the standard Fr distribution, while capable of modeling heavy tails, often fails to reflect the nuanced behavior of real financial and insurance data. It assumes a fixed tail decay rate governed solely by a single shape parameter, which cannot capture shifts in tail risk driven by market regimes, policy interventions, or structural breaks. In housing markets, for instance, price extremes are influenced by localized supply constraints, zoning laws, or speculative bubble factors that induce heterogeneity in tail behavior not accommodated by the rigid Fréchet form. Similarly, in reinsurance, large losses arise from complex, clustered catastrophes whose severity and frequency evolve over time, yet the standard Fréchet treats all extremes as identically distributed beyond a threshold. This inflexibility leads to biased risk assessments, particularly in VaR and ExSh estimates, which are critical for capital adequacy and solvency. Moreover, the inability to adjust tail thickness in response to changing economic conditions undermines dynamic risk management and regulatory stress testing. Consequently, relying on the classical Fréchet may result in undercapitalization during systemic

stress or mispricing of extreme-event-linked instruments. These shortcomings highlight the need for a more adaptive model that preserves the heavy-tailed foundation while embedding economic realism into its tail structure. The proposed LAPFr distribution addresses this gap by introducing additional shape flexibility that better aligns with observed economic dynamics in extreme outcomes. Thus, our contribution bridges a critical disconnect between theoretical tail modeling and practical economic risk assessment. By inserting (2) in (1), we get CDF of the LAPFr model, which can be expressed as

$$F(x,\Psi) = C\,log\left\{1+exp\left[-\left(\frac{\alpha}{x}\right)^{\theta}\right]\right\}exp\left\{\beta exp\left[-\left(\frac{\alpha}{x}\right)^{\theta}\right]\right\}, x>0, \tag{3}$$

where $\Psi=(\beta,\alpha,\theta)$. The bivariate version of (3) can be derived according to [2,3] and be used for more bivariate financial applications. Starting with (3), the corresponding PDF of the LAPFr model can be derived as:

$$f(x;\boldsymbol{\Psi}) = C\theta\alpha^{\theta}x^{-\theta-1}exp\left[-\left(\frac{\alpha}{x}\right)^{\theta}\right]exp\left\{\beta exp\left[-\left(\frac{\alpha}{x}\right)^{\theta}\right]\right\}p(x;\boldsymbol{\Psi}), x>0, \tag{4}$$

where

$$p(x;\boldsymbol{\Psi}) = \frac{1}{1+exp\left[-\left(\frac{\alpha}{x}\right)^{\theta}\right]} + \beta\,log\left\{1+exp\left[-\left(\frac{\alpha}{x}\right)^{\theta}\right]\right\}.$$

A key feature of this family lies in the structure of the PDF, where the exponential term $exp\left\{\beta exp\left[-\left(\frac{\alpha}{x}\right)^{\theta}\right]\right\}$ introduces a form of exponential weighting dependent on the baseline CDF. As $x\to-\infty$, $exp\left[-\left(\frac{\alpha}{x}\right)^{\theta}\right]\to 0$,

$$log\left[1+exp\left[-\left(\frac{\alpha}{x}\right)^{\theta}\right]\right] \approx exp\left[-\left(\frac{\alpha}{x}\right)^{\theta}\right], exp\left\{\beta exp\left[-\left(\frac{\alpha}{x}\right)^{\theta}\right]\right\} \approx 1+\beta exp\left[-\left(\frac{\alpha}{x}\right)^{\theta}\right].$$

Then,

$$F(x;\boldsymbol{\Psi}) \approx Cexp\left[-\left(\frac{\alpha}{x}\right)^{\theta}\right]\left[1+\beta exp\left[-\left(\frac{\alpha}{x}\right)^{\theta}\right]\right] \to 0 \text{ as } x\to-\infty.$$

As $x\to+\infty$, $exp\left[-\left(\frac{\alpha}{x}\right)^{\theta}\right]\to 1$,

$$log\left[1+exp\left[-\left(\frac{\alpha}{x}\right)^{\theta}\right]\right] \approx log(2), exp\left\{\beta exp\left[-\left(\frac{\alpha}{x}\right)^{\theta}\right]\right\} \approx e^{\beta}.$$

Then,

$$F(x;\boldsymbol{\Psi}) \approx C\,log(2)\,e^{\beta} = 1 \text{ as } x\to+\infty.$$

As $x\to-\infty$, $f(x;\boldsymbol{\Psi})\to 0$. As $x\to+\infty$, $f(x;\boldsymbol{\Psi})\to 0$.

Even though the LAPFr model introduces additional structure via $exp\left\{\beta exp\left[-\left(\frac{\alpha}{x}\right)^{\theta}\right]\right\}$ and $p(x;\boldsymbol{\Psi})$, all these terms tend to constant as $x \to +\infty$. Therefore, they do not affect the power-law decay rate. Hence, the survival function of the LAPFr model still satisfies:

$$P(X > x) \sim \left(\frac{1}{x}\right)^{\theta} \; as \; x \to +\infty.$$

This means the tail index remains θ, the same as the baseline Fr distribution. This is because the survival function decays asymptotically as $\left(\frac{1}{x}\right)^{\theta}$, characteristic of a Fr-type distribution. Despite the added complexity from the log-adjusted polynomial structure, the tail behavior is dominated by the underlying Fréchet kernel, and thus the tail index remains unchanged at θ.

In this paper, a suite of actuarial risk measures is employed to evaluate the performance of the LAPFr model, including VaR, ExSh, TV, TMV, MOO^{P}, and the PORT-VaR methodology. The PORT-VaR approach allows for a detailed examination of exceedances over high quantile thresholds, providing insights into the frequency and severity of extreme observations across varying confidence levels. The results indicate that both datasets exhibit pronounced heavy-tailed characteristics, with a significant number of exceedances observed even at high confidence levels, reinforcing the necessity of using models specifically designed for extreme value analysis. Furthermore, the MOO^{P} analysis reveals that increasing the number of top-order observations included in the average leads to a reduction in estimation bias and mean squared error, suggesting improved stability in tail estimation with larger P values, with P = 10 emerging as a practical choice for optimal performance. The RAROC metric is applied to assess the trade-off between return and tail risk, offering a practical perspective for risk managers and financial institutions. The findings show a consistent decline in RAROC as confidence levels increase, indicating that the efficiency of returns deteriorates under extreme scenarios. This has critical implications for capital allocation, solvency assessment, and regulatory compliance, particularly in sectors exposed to rare but high-impact events. One-step-ahead VaR forecasting further illustrates the model's predictive capability, although the observed decrease in expected average excess loss (EAEL) at higher quantiles warrants careful interpretation. This counterintuitive trend may reflect data truncation, model limitations, or structural constraints within the systems under study, highlighting the importance of complementing VaR with more sensitive tail measures such as expected shortfall.

2. Properties

2.1. Alternative expansions

By expanding $exp\left\{\beta exp\left[-\left(\frac{\alpha}{x}\right)^{\theta}\right]\right\}$, the new CDF can be expressed as

$$F(x;\boldsymbol{\Psi}) = C\, log\left\{1 + exp\left[-\left(\frac{\alpha}{x}\right)^{\theta}\right]\right\}\sum_{\tau=0}^{+\infty}\frac{\beta^{\tau}}{\tau!}\left\{exp\left[-\left(\frac{\alpha}{x}\right)^{\theta}\right]\right\}^{\tau}, x > 0. \quad (5)$$

Then, by expanding $log\left\{1 + exp\left[-\left(\frac{\alpha}{x}\right)^{\theta}\right]\right\}$, we have

$$log\left\{1+exp\left[-\left(\frac{\alpha}{x}\right)^{\theta}\right]\right\}=\sum_{\hbar=1}^{+\infty}\frac{(-1)^{1+\hbar}}{\hbar!}\left\{exp\left[-\left(\frac{\alpha}{x}\right)^{\theta}\right]\right\}^{\hbar}. \quad (6)$$

Inserting (6) into (5), the new CDF can be simplified as

$$F(x;\boldsymbol{\Psi})=\sum_{\tau=0}^{+\infty}\sum_{\hbar=1}^{+\infty}d_{\tau,\hbar}\,W_{\tau,\hbar}(x;\alpha,\theta),x>0, \quad (7)$$

where

$$d_{\tau,\hbar}=\frac{C}{\tau!\,\hbar!}(-1)^{1+\tau}\beta^{\tau},$$

and $W_{\tau,\hbar}(x;\alpha,\theta)=exp\left[-(\tau+\hbar)\left(\frac{\alpha}{x}\right)^{\theta}\right]$ refers to the CDF of the Fr model with scale parameter $\alpha(\tau+\hbar)^{\frac{1}{\theta}}$ and shape parameter θ. By differentiating (7), we have

$$f(x;\boldsymbol{\Psi})=\sum_{\tau=0}^{+\infty}\sum_{\hbar=1}^{+\infty}d_{\tau,\hbar}\,w_{\tau,\hbar}(x;\alpha,\theta),x>0, \quad (8)$$

where

$$w_{\tau,\hbar}(x;\alpha,\theta)=dW_{\tau,\hbar}(x;\alpha,\theta)/dx=(\tau+\hbar)\theta\alpha^{\theta}x^{-\theta-1}exp\left[-(\tau+\hbar)\left(\frac{\alpha}{x}\right)^{\theta}\right], \quad (9)$$

which refers to the PDF of the Fr model with scale parameter $\alpha(\tau+\hbar)^{\frac{1}{\theta}}$ and shape parameter θ. To summarize, we say that Eq (8) can be used to derive most of the mathematical properties of the underlying distribution to be studied.

2.2. Moments

Let $Y_{\tau,\hbar}$ be a random variable having density in (4). Then, the r^{th} ordinary moment of X, say μ_r', follows from (8) as

$$\mu_r'=E(X^r)=\sum_{\tau=0}^{+\infty}\sum_{\hbar=1}^{+\infty}\left[d_{\tau,\hbar}\,E\left(Y_{\tau,\hbar}^{r}\right)\right],$$

where

$$E\left(Y_{\tau,\hbar}^{r}\right)=(\tau+\hbar)\int_{-\infty}^{\infty}x^{r}\;(\tau+\hbar)\theta\alpha^{\theta}x^{-\theta-1}exp\left[-(\tau+\hbar)\left(\frac{\alpha}{x}\right)^{\theta}\right]dx=\alpha^{r}(\tau+\hbar)^{\frac{r}{\theta}}\Gamma\left(1-\frac{r}{\theta}\right),$$

where

$$\Gamma(a,)=\int_{0}^{+\infty}y^{a-1}\,exp(y)dy.$$

Then,

$$\mu_r'=E(X^r)=\sum_{\tau=0}^{+\infty}\sum_{\hbar=1}^{+\infty}d_{\tau,\hbar}\;\alpha^{r}(\tau+\hbar)^{\frac{r}{\theta}}\Gamma\left(1-\frac{r}{\theta}\right). \quad (10)$$

Setting $r = 1$ in (10) gives the mean of X. We acknowledge that this domain of existence was not explicitly stated in the manuscript and will clarify in revision that the r[th] moment exists if and only if $r < \theta$, consistent with the tail index preservation property highlighted in Section 1.

2.3. Incomplete moments

The r^{th} incomplete moment of X is given by

$$m_{r,X}(t) = \int_{-\infty}^{t} x^r f(x; \boldsymbol{\Psi}) dx.$$

Using (8), the r^{th} incomplete moment of LAP family is

$$m_{r,X}(t) = \sum_{\tau=0}^{+\infty} \sum_{k=1}^{+\infty} d_{\tau,k} m_{r,\tau+k,X}(t),$$

where

$$m_{r,\tau+k,X}(t) = \int_{-\infty}^{t} x^r w_{\tau,k}(x; \alpha, \theta) dx = \alpha^r (\tau + k)^{\frac{r}{\theta}} \gamma\left(1 - \frac{r}{\theta}, (\tau + k)\left(\frac{\alpha}{t}\right)^{\theta}\right).$$

Then,

$$m_{r,X}(t) = \sum_{\tau=0}^{+\infty} \sum_{k=1}^{+\infty} d_{\tau,k} \alpha^r (\tau + k)^{\frac{r}{\theta}} \gamma\left(1 - \frac{r}{\theta}, (\tau + k)\left(\frac{\alpha}{t}\right)^{\theta}\right), \tag{11}$$

where $\gamma(a, z) = \int_0^z y^{a-1} exp(y) dy$ is the lower incomplete moments.

2.4. Moment generating function

The moment generating function (MGF) of X, say $M(t) = E(e^{tX})$, is obtained from (8) as

$$M(t) = \sum_{\tau=0}^{+\infty} \sum_{k=1}^{+\infty} \left[d_{\tau,k} M_{\tau+k}(t)\right],$$

where $M_{\tau+k}(t)$ is the generating function of $Y_{\tau+k}$ given by

$$M_{\tau+k}(t) = (\tau + k) \int_{-\infty}^{\infty} e^{tx} w_{\tau,k}(x; \alpha, \theta) dx = \sum_{r=0}^{+\infty} \frac{t^r}{r!} \alpha^r (\tau + k)^{\frac{r}{\theta}} \Gamma\left(1 - \frac{r}{\theta}\right).$$

Then,

$$M(t) = \sum_{\tau=0}^{+\infty} \sum_{k=1}^{+\infty} \sum_{r=0}^{+\infty} d_{\tau,k} \frac{t^r}{r!} \alpha^r (\tau + k)^{\frac{r}{\theta}} \Gamma\left(1 - \frac{r}{\theta}\right). \tag{12}$$

3. Actuarial indicators

3.1. The VaR indicator

According to [4], the VaR indicator is a widely used risk measure that quantifies the maximum potential losses over a given time horizon at a specified confidence level (CL). For the proposed LAPFr model, the VaR at CL $q \in (0,1)$ is derived directly from the quantile function of the distribution. The quantile function (qf) of X can be determined by inverting $F(x) = q$ in (1), where

$$qe^{\beta}\, log(2) = log\left[1 + exp\left[-\left(\frac{\alpha}{x}\right)^{\theta}\right]\right] exp\left\{\beta exp\left[-\left(\frac{\alpha}{x}\right)^{\theta}\right]\right\},$$

then

$$qe^{\beta}\, log(2) = log\left(1 + exp\left[-\left(\frac{\alpha}{x}\right)^{\theta}\right]\right) exp\left\{\beta exp\left[-\left(\frac{\alpha}{x}\right)^{\theta}\right]\right\}.$$

For small values of $exp\left[-\left(\frac{\alpha}{x}\right)^{\theta}\right]$, we can approximate $log\left(1 + exp\left[-\left(\frac{\alpha}{x}\right)^{\theta}\right]\right) \approx exp\left[-\left(\frac{\alpha}{x}\right)^{\theta}\right]$, so

$$q\beta e^{\beta}\, log(2) = \beta exp\left[-\left(\frac{\alpha}{x}\right)^{\theta}\right] exp\left\{\beta exp\left[-\left(\frac{\alpha}{x}\right)^{\theta}\right]\right\}.$$

Following [5], and letting $z(\beta, \alpha, \theta) = \beta exp\left[-\left(\frac{\alpha}{x}\right)^{\theta}\right]$, and then using Lambert $\boldsymbol{W}[.]$,

$$q\beta e^{\beta}\, log(2) = z(\beta, \alpha, \theta) e^{z(\beta,\alpha,\theta)} \Rightarrow z(\beta, \alpha, \theta) = \boldsymbol{W}\left(q\beta e^{\beta}\, log(2)\right) \Rightarrow \beta exp\left[-\left(\frac{\alpha}{x}\right)^{\theta}\right] = \boldsymbol{W}\left[q\beta e^{\beta}\, log(2)\right]$$

$$\Rightarrow exp\left[-\left(\frac{\alpha}{x}\right)^{\theta}\right] = \frac{1}{\beta}\boldsymbol{W}\left[q\beta e^{\beta}\, log(2)\right] \Rightarrow exp\left[-\left(\frac{\alpha}{x}\right)^{\theta}\right] = \frac{1}{\beta}\boldsymbol{W}\left[q\beta e^{\beta}\, log(2)\right].$$

Then,

$$x_q = G^{-1}\left\{\frac{1}{\beta}\boldsymbol{W}\left[q\beta e^{\beta}\, log(2)\right]; \alpha, \theta\right\}. \tag{13}$$

Using Eq (13) from the manuscript, the VaR is given by:

$$VaR = VaRq = Q(q) = \alpha\left(-\ln\left\{\frac{1}{\beta}\boldsymbol{W}\left[q\beta e^{\beta}\, log(2)\right]\right\}\right)^{-\frac{1}{\theta}}.$$

The flexibility of the new LAPFr model allows for improved modeling of the heavy-tailed insurance, financial and economic datasets, as demonstrated in the analysis of insurance, reinsurance revenues and housing prices (see [6]). Indeed, Eq (13) employs the asymptotic approximation

$\log(1+e^{-u}) \approx e^{-u}$ for large u (i.e., in the far tail where $G(x) \to 1$ and $u = -logG(x) \to 0^{+}$), which enables a tractable Lambert-*W* inversion. This is an asymptotic approximation, not an exact quantile expression, and we acknowledge that the manuscript did not explicitly label it as such. The approximation is valid when $e^{-u} \ll 1$, i.e., for high confidence levels (typically $q \geq 0.90$), where tail risk analysis is most relevant.

3.2. The ExSh indicator

The ExSh (or tail value-at-risk (ExSh)) (see [7]), measures the expected loss given that the loss exceeds the VaR threshold at CL q. For the proposed LAPFr model, the ExSh at CL q is defined as:

$$\text{ExSh} = \text{ExSh}q = E[\, X \mid X > VaRq \,].$$

Using the first incomplete moment of the distribution (from Eq (11)), this can be expressed as:

$$\text{ExSh} = \sum_{\tau=0}^{+\infty}\sum_{\hbar=1}^{+\infty} d_{\tau,\hbar}\alpha(\tau+\hbar)^{\frac{1}{\theta}}\Gamma\left(1-\frac{1}{\theta},(\tau+\hbar)\left(\frac{\alpha}{t}\right)^{\theta}\right), \tag{15}$$

where

$$\Gamma\left(1-\frac{1}{\theta},(\tau+\hbar)\left(\frac{\alpha}{t}\right)^{\theta}\right) = \Gamma\left(1-\frac{1}{\theta}\right) - \gamma\left(1-\frac{1}{\theta},(\tau+\hbar)\left(\frac{\alpha}{t}\right)^{\theta}\right).$$

3.3. The TV indicator

For a random variable $X \sim$ LAPFr, the TV at CL q is defined as:

$$\text{TV}q = \text{E}(X^2 | X > VaRq) - (\text{ExSh}q)^2.$$

Then,

$$\text{TV}q = \sum_{\tau=0}^{+\infty}\sum_{\hbar=1}^{+\infty} d_{\tau,\hbar}\,\alpha^2(\tau+\hbar)^{\frac{2}{\theta}}\gamma\left(1-\frac{2}{\theta},(\tau+\hbar)\left(\frac{\alpha}{t}\right)^{\theta}\right) - \left[\sum_{\tau=0}^{+\infty}\sum_{\hbar=1}^{+\infty} d_{\tau,\hbar}\alpha(\tau+\hbar)^{\frac{1}{\theta}}\Gamma\left(1-\frac{1}{\theta},(\tau+\hbar)\left(\frac{\alpha}{t}\right)^{\theta}\right)\right]^2. \tag{16}$$

3.4. Tke TMV indicator

The TMV is a composite risk indicator that combines the expected value (ExV) and variability of losses in the tail region of a certain distribution. It provides a more complete result of tail risk by incorporating both central tendency and dispersion. The TMV (see [8]) can be expressed as

$$\text{TMV}q = \text{ExSh}q + c\sqrt{\text{TV}q},$$

where $c \geq 0$ is a risk-aversion parameter reflecting the decision-maker's sensitivity to uncertainty in the tail. A higher c leads to a more conservative risk assessment. Then,

$$\mathrm{TMV}q = \sum_{\tau=0}^{+\infty}\sum_{\hbar=1}^{+\infty} d_{\tau,\hbar}\frac{\alpha}{(\tau+\hbar)^{-\frac{1}{\theta}}}\Gamma\left(1-\frac{1}{\theta},(\tau+\hbar)\left(\frac{\alpha}{t}\right)^{\theta}\right)$$
$$+c\sqrt{\begin{array}{l}\sum_{\tau=0}^{+\infty}\sum_{\hbar=1}^{+\infty} d_{\tau,\hbar}\frac{\alpha^2}{(\tau+\hbar)^{-\frac{2}{\theta}}}\gamma\left(1-\frac{2}{\theta},(\tau+\hbar)\left(\frac{\alpha}{t}\right)^{\theta}\right)\\ -\left[\sum_{\tau=0}^{+\infty}\sum_{\hbar=1}^{+\infty} d_{\tau,\hbar}\frac{\alpha}{(\tau+\hbar)^{-\frac{1}{\theta}}}\Gamma\left(1-\frac{1}{\theta},(\tau+\hbar)\left(\frac{\alpha}{t}\right)^{\theta}\right)\right]^2\end{array}}. \tag{17}$$

3.5. The RAROC indicator

Due to [9], RAROC is a risk management metric used to assess the profitability of a business or investment relative to the risk involved. It is calculated as the ratio of the risk-adjusted return (RAR) to the VaR. Then,

$$\mathrm{RAROC} = \mathrm{RAROC}\left(q;\widehat{\boldsymbol{\Psi}}\right) = \frac{1}{\mathrm{VaR}\left(q;\widehat{\boldsymbol{\Psi}}\right)}\mathrm{Ex}(\mathrm{R},\mathrm{L},q|\widehat{\boldsymbol{\Psi}}), \tag{18}$$

where $\mathrm{Ex}(\mathrm{R},\mathrm{L},q|\widehat{\boldsymbol{\Psi}})$ refers to the RAR, which is the expected return adjusted for the risk associated with the investment. The RAR is typically the expected return from an investment minus the expected loss due to risk. If you have the expected return $\mathrm{Ex}\left(\mathrm{R};q|\widehat{\boldsymbol{\Psi}}\right)$ and expected loss $\mathrm{EX}\left(\mathrm{L};q|\widehat{\boldsymbol{\Psi}}\right)$, the RAR can be written as

$$\mathrm{RAR} = \mathrm{Ex}(\mathrm{R},\mathrm{L},q|\widehat{\boldsymbol{\Psi}}) = \mathrm{Ex}\left(\mathrm{R};q|\widehat{\boldsymbol{\Psi}}\right) - \mathrm{Ex}\left(\mathrm{L};q|\widehat{\boldsymbol{\Psi}}\right). \tag{19}$$

Now, we can combine the two to compute the $\mathrm{RAROC}\left(q;\widehat{\boldsymbol{\Psi}}\right)$ for the LAPFr model as

$$\mathrm{RAROC}\left(q;\widehat{\boldsymbol{\Psi}}\right) = \frac{1}{\alpha}\left(-\ln\left\{\frac{1}{\beta}\mathbf{W}\left[q\beta e^{\beta}\,log(2)\right]\right\}\right)^{\frac{1}{\theta}}\mathrm{Ex}(\mathrm{R},\mathrm{L},q|\widehat{\boldsymbol{\Psi}}). \tag{20}$$

3.6. The MOO^P indicator

MOOP is a robust statistical measure used to analyze extreme values in a dataset by focusing on the largest observations. It is particularly useful in financial and actuarial risk analysis for assessing tail behavior and quantifying the severity of extreme events. MOOP is calculated as the arithmetic mean of the P largest values in a dataset, where P is a positive integer ranging from 1 to the total number of observations. For a random sample of size n, let $X_{(1)}$, $X_{(2)}$, …, $X_{(n)}$ denote the order statistics, with $X_{(n)}$ being the largest value. Then, the MOO$^{\mathrm{P}}$ at order P is defined as:

$$\mathrm{MOO}^{\mathrm{P}} = \frac{1}{P}\sum_{i=1}^{p} X_{(n-i+1)}. \tag{21}$$

This formula computes the average of the top P extreme values. As P increases, more data points from the upper tail are included in the average, which can improve estimation stability (see [10] for more reliability MOO$^{\mathrm{P}}$ applications).

3.7. The PORT-VaR method

According to [11], the PORT-VaR method is computed by first selecting a high quantile threshold uq corresponding to a CL q. Exceedances over this threshold are identified as extreme values. The number and magnitude of these peaks are analyzed to assess tail risk. For each q, the VaR is calculated using the quantile function of the LAPFr model (Eq 9); then peaks above it are extracted. Summary statistics (min, mean, max, etc.) of the peaks are computed, as shown below (see [12] for more applications and [13,14] for more real related data). The algorithms below can be used to obtain the PORT-VAR:

Algorithm 1. Choose a CL q.
Algorithm 2. Compute VaRq using quantile function (see Eq 9).
Algorithm 3. Identify all data points exceeding VaRq.
Algorithm 4. These exceedances are the "peaks" above the threshold.
Algorithm 5. Count the number of peaks.
Algorithm 6. Calculate their mean, median, min, max, and quartiles.
Algorithm 7. Analyze peak behavior across increasing q levels.

4. Risk analysis under the LAPFr model

The first dataset in this study includes the median housing prices (MHP) for 506 neighborhoods in Boston (see [15]). The second dataset is related to U.S. reinsurance financial revenues data (see [16–18] for more insurance applications under risk analysis). The current datasets are now explicitly labeled as example 1 (Boston Housing Prices) and example 2 (U.S. reinsurance financial revenues data). Each example is used to validate specific aspects of the model, such as the tail index and risk measures including the VaR, ExSh, TMV, TV, MOO^{P}, PORT-VaR, and RAROC.

4.1. Risk analysis under the extreme prices data

4.1.1. Empirical MOO^{P} assessment under the extreme prices data

In this section, we carry out an economic analysis of the extreme prices data using the MOO^{P} and PORT-VaR methodologies (refer to [16]). We begin with a graphical exploration of the dataset, as illustrated in Figure 1, which presents several visual tools, boxplot, kernel density plot, QQ plot, and violin plot, each offering valuable perspectives on the data's structure and behavior.

The boxplot provides a clear summary of the data through its five-number statistics: minimum, first quartile, median, third quartile, and maximum. It also highlights potential outliers. For the Boston housing data, we notice a considerable number of high-value outliers, indicating neighborhoods with unusually expensive homes. These upper-end extremes can distort the overall distribution and suggest significant variability in housing costs across areas. The distance between quartiles further reflects the spread and dispersion in prices. Next, the kernel density plot offers a smooth, continuous representation of the price distribution, unlike the binning approach of a histogram. In this case, the plot shows a right-skewed distribution, which is common in housing markets: while most homes are priced in the low to moderate range, a smaller number of high-end properties extend the right tail.

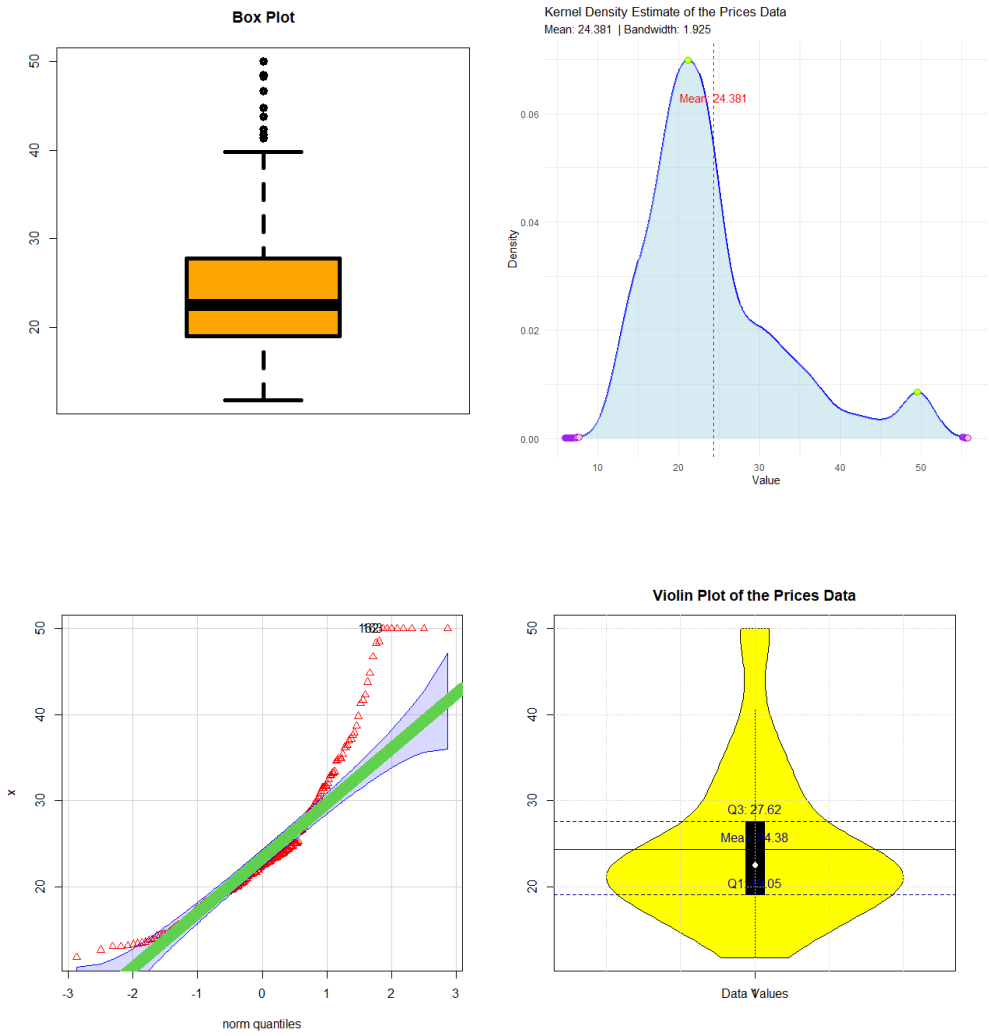

Figure 1. Graphs describing the housing prices data.

The QQ plot compares the quantiles of our data against those of a theoretical normal distribution. If the data were normally distributed, the points would align closely with a straight line. However, in the Boston housing dataset, we observe clear deviations, especially in the upper quantiles, confirming the presence of heavy tails and extreme values, a common trait in economic and financial datasets. Finally, the violin plot combines the features of both the boxplot and the density plot, illustrating not only summary statistics but also the shape of the distribution. Here, it reveals that most house prices cluster in the lower range, with a long tail trailing toward higher values. This pattern may also hint at multimodality, a possible evidence of different housing market segments, such as average versus luxury homes, giving deeper insight into the underlying economic landscape.

Following this, we conduct an economic risk assessment using the MOO^P and PORT-VaR approaches. Table 1 presents the results of the MOO^P analysis for values of P ranging from 1 to 20, along with the corresponding mean squared error (MSE) and bias. The results show that as P increases, the estimates become more precise, with both MSE and bias gradually decreasing. This suggests that including more extreme observations in the average leads to a more stable and less

biased estimation of tail behavior. However, it's important to carefully assess performance beyond P = 10, as the rate of improvement may slow down, and further increasing P could lead to diminishing returns or even overfitting.

Table 1. MSE and bias for assessing the MOO^P under P=1, 2, 3, …, 20 for the prices data.

P| TM	1,2,3,4,5 | 23.61976
MOO^P	5.983333, 6.157143, 6.2875, 6.388889, 6.49
MSE	311.0436, 304.943, 300.4073, 296.903, 293.4288
Bias	18.6198, 18.61976, 18.4198, 18.14476, 17.83976
P| TM	6,7,8,9,10 | 23.61976
MOO^P	5.983333, 6.157143, 6.2875, 6.388889, 6.49
MSE	311.0436, 304.943, 300.4073, 296.903, 293.4288
Bias	17.63643, 17.4626, 17.33226, 17.23087, 17.12976
P| TM	11,12,13,14,15 | 23.61976
MOO^P	6.581818, 6.708, 6.830769, 6.9357, 7.033333,
MSE	290.292, 285.996, 281.87, 278.3575, 275.1096,
Bias	17.0379, 16.9114, 16.7889, 16.68405, 16.5864
P| TM	16,17,18,19,20 | 23.61976
MOO^P	7.11875, 7.2, 7.27, 7.347368, 7.42, 7.485714, 7.57727
MSE	272.2834, 269.6086, 267.2421, 264.7908, 262.4323
Bias	16.5, 16.41976, 16.34754, 16.27239, 16.19976

As P grows from 1 to 20, the MOO^P values themselves rise steadily, which is expected since we're averaging over progressively larger sets of high values. The declining MSE and bias confirm that the estimator becomes more accurate and reliable with higher P, at least up to a certain point. The most notable improvements occur between P = 1 and P = 10, after which the gains in accuracy begin to taper off.

Choosing the optimal value of P (OPT-P) requires balancing model accuracy against complexity. Ideally, we want a P that minimizes error without unnecessarily increasing the number of parameters. A reasonable strategy is to select the P where MSE reaches its lowest point while bias remains acceptably small. Based on the trend in the data, P = 10 appears to be a strong candidate for OPT-P, as it captures significant accuracy gains without pushing into the range of marginal improvements. Ultimately, the final choice can be fine-tuned depending on the specific goals of the analysis and visual inspection of the results.

Figure 2 illustrates the MOO^P values across different P levels for the dataset on U.S. reinsurance financial revenues (measured in thousands of dollars). Here, MOO^P is computed as the average of the top P observations for each P, allowing us to track how the estimated tail mean evolves as more extreme values are included.

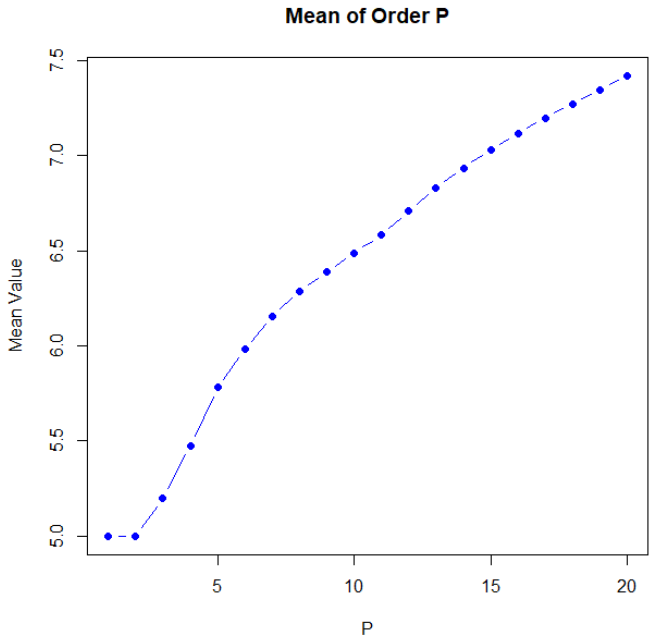

Figure 2. The MOO^P for the prices data.

4.1.2. Peaks above VaR threshold analysis for prices data

Table 2 presents a PORT-VaR analysis for the Boston housing prices dataset across six different confidence levels (75% to 99%). It shows how risk measures change as the threshold for extreme values becomes more stringent. The table includes key indicators like VaR, ExSh, TV, and TMV, along with the number of data points exceeding each VaR threshold. As the confidence level increases, the VaR rises, reflecting higher thresholds for what's considered an extreme price. Interestingly, ExSh decreases slightly, which suggests that while the threshold goes up, the average of exceedances stabilizes. The number of peaks above VaR grows from 379 at 75% to all 506 observations at 99%, showing how inclusive the threshold becomes. Summary statistics of the peak minimum, quartiles, mean, and maximum, are also provided, giving insight into the distribution of extreme values. At lower confidence levels, the peaks are more dispersed, but as the threshold tightens, only the highest values remain. The decreasing trend in ExSh and fluctuating TMV indicate changing tail behavior under different thresholds. The large number of exceedances, even at high confidence levels, highlights the heavy-tailed nature of housing prices. This aligns with real expectations where a few neighborhoods have significantly higher prices. The results support the use of extreme value theory in modeling such economic data.

As the confidence level rises from 75% to 99%, the VaR threshold increases sharply, reflecting a growing expectation of extreme price events in high-end real estate markets. The declining ExSh suggests that while thresholds rise, the average severity of exceedances stabilizes, which may indicate market saturation at the top end. This pattern is typical in housing markets where a few luxury properties skew the upper tail without significantly altering the average risk profile. The increasing number of peaks above VaR—from 379 to 500—shows that a large portion of the dataset consists of relatively high values, reinforcing the idea of a market with widespread appreciation but

concentrated extremes. The rising TV confirms growing volatility in the upper tail, signaling higher uncertainty for investors or insurers exposed to these segments. The TMV, which combines mean and variance, fluctuates but remains substantial, indicating persistent risk even after adjusting for risk aversion. Economically, this reflects structural imbalances in housing supply and demand, especially in urban areas like Boston. For risk managers, these results highlight the importance of preparing for frequent extreme values rather than rare, isolated shocks. The data supports the use of advanced tail modeling in real estate risk assessment, particularly for mortgage insurers or portfolio managers. From a policy standpoint, the heavy-tailed nature of prices may call for target interventions to improve market stability.

Table 2. PORT-VaR analysis for prices data under the LAPFr model.

CL	VaR	ExSh	TV	TMV	Number of peaks above VaR threshold	Min., 1st Qu., Med., Mean, 3rd Qu., Max.,
75%	27.50	25.82	42.00	39.18	379	17.10, 20.25, 23.10, 25.82, 28.70, 50.00
80%	29.84	25.20	61.21	39.68	405	15.30, 19.70, 22.70, 25.20, 28.20, 50.00
85%	32.61	24.58	101.33	36.85	430	14.00, 19.30, 22.30, 24.58, 27.50, 50.00
90%	36.07	23.97	181.23	34.82	455	12.80, 18.70, 22.00, 23.97, 26.65, 50.00
95%	45.31	23.35	521.42	39.18	479	10.40, 17.85, 21.70, 23.35, 26.30, 50.00
99%	50.00	22.73	777.00	33.35	500	7.20, 17.20, 21.30, 22.73, 25.00, 50.00

Figure 3 gives the histogram of prices with peaks and VaR under some CLs for prices data. Figure 4 shows the corresponding Kernel densities of prices with peaks and VaR under some CLs for prices data.

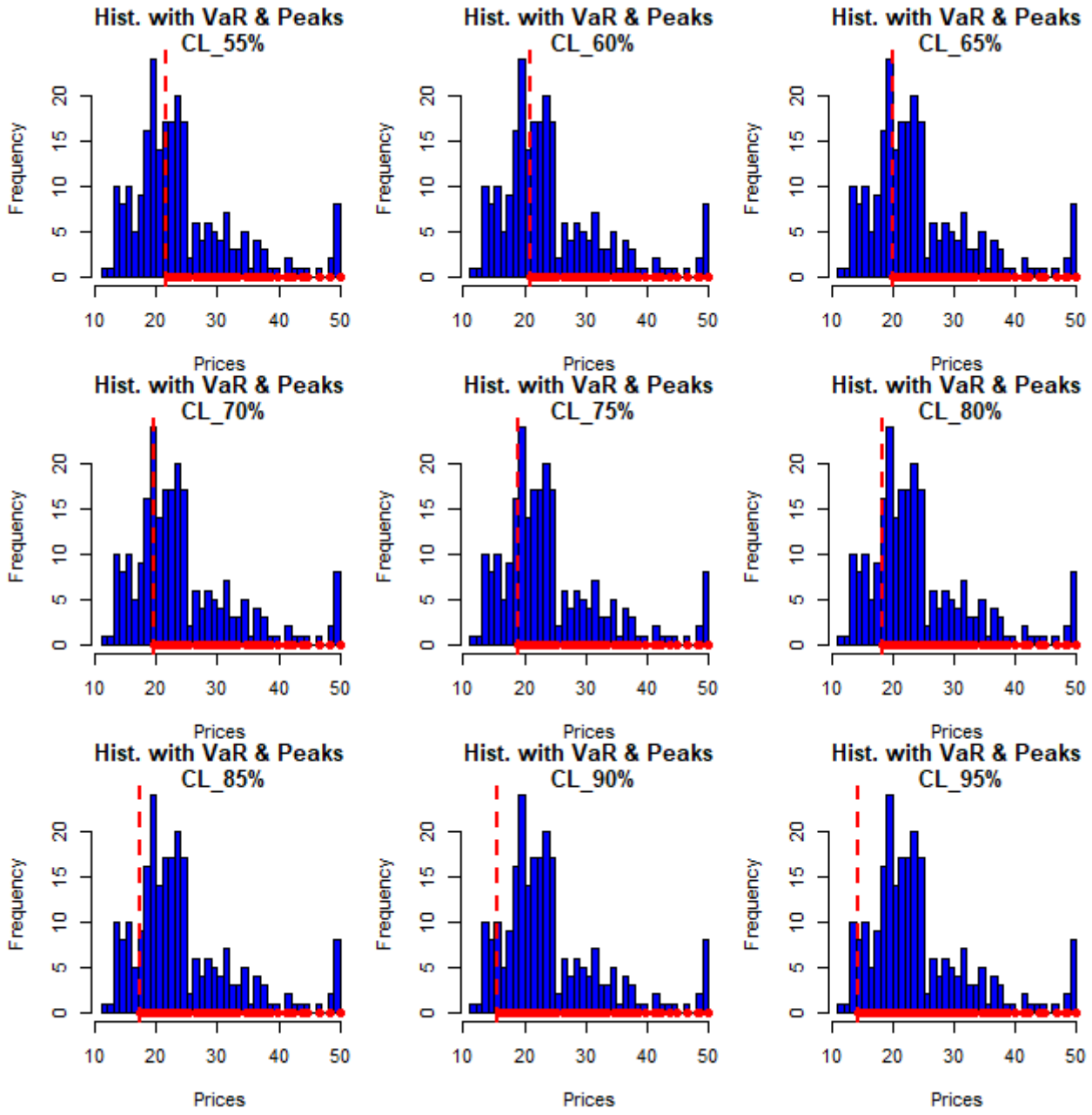

Figure 3. Histogram of prices with peaks and VaR under some CLs for prices data.

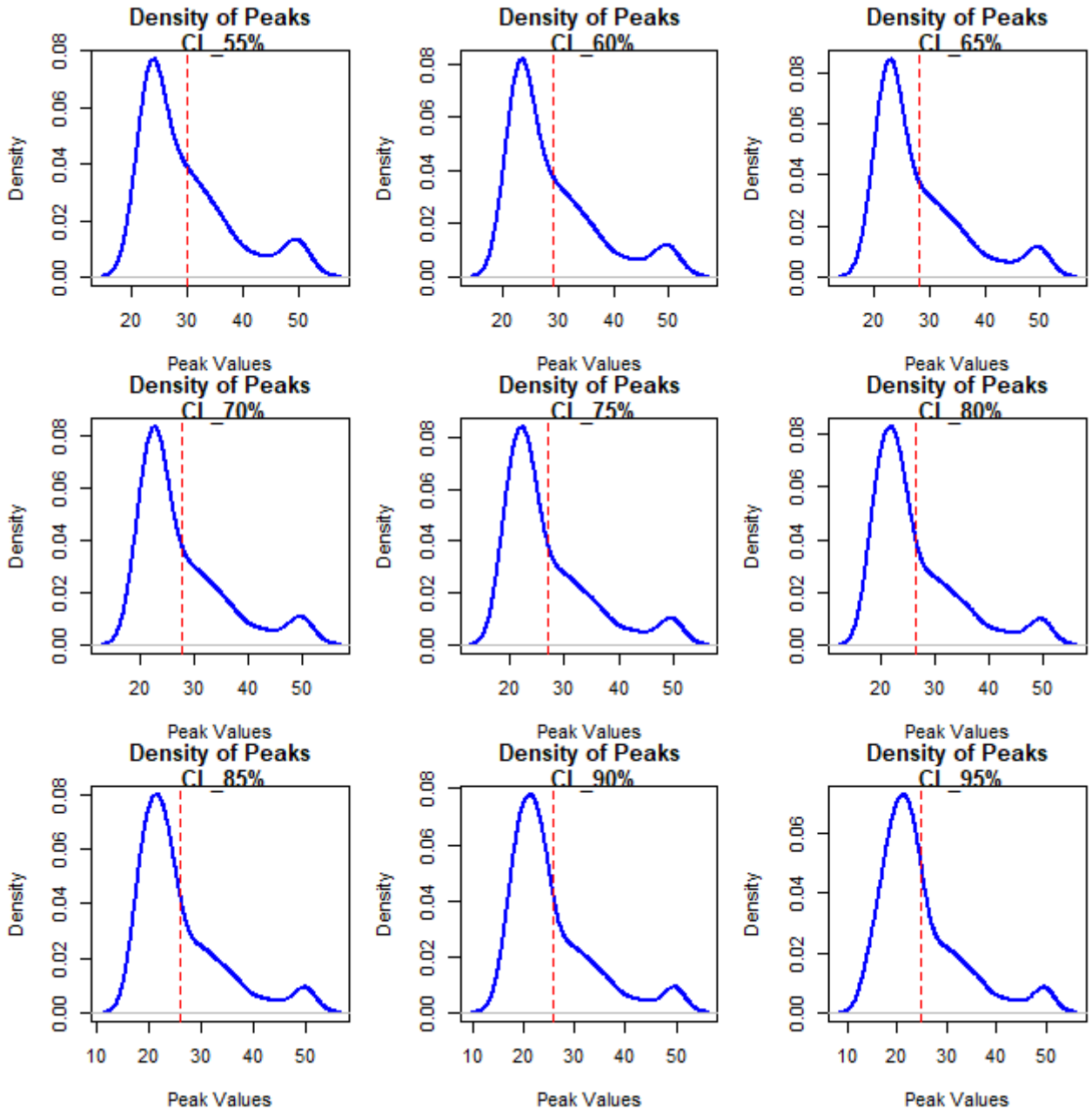

Figure 4. Kernel densities of prices with peaks and VaR under some CLs for prices data.

4.2. Risk analysis under the financial reinsurance revenue data

4.2.1. Empirical MOO^{P} assessment under the financial reinsurance revenue data

This section delves into the reinsurance revenue of a reinsurance company operating within the United States insurance industry, with a specific focus on analyzing recent time series data. Reinsurance plays a pivotal role in the broader insurance ecosystem, acting as a safety net for primary insurance companies by spreading the risk associated with underwriting large policies. The reinsurance sector is thus a key element in maintaining the stability and financial health of the overall insurance industry. The data used in this study is publicly available via the United States

government's data.gov portal (*https://catalog.data.gov/dataset*), which hosts an array of datasets, including those related to insurance and reinsurance sectors. Figure 5 below describes revenue data. Figure 6 provides the TM vs. the MOO^P for the revenue data. Table 3 presents the MSE and Bias for assessing the MOOP under P=1, 2, 3, …, 20 for the for the U.S. financial reinsurance revenue.

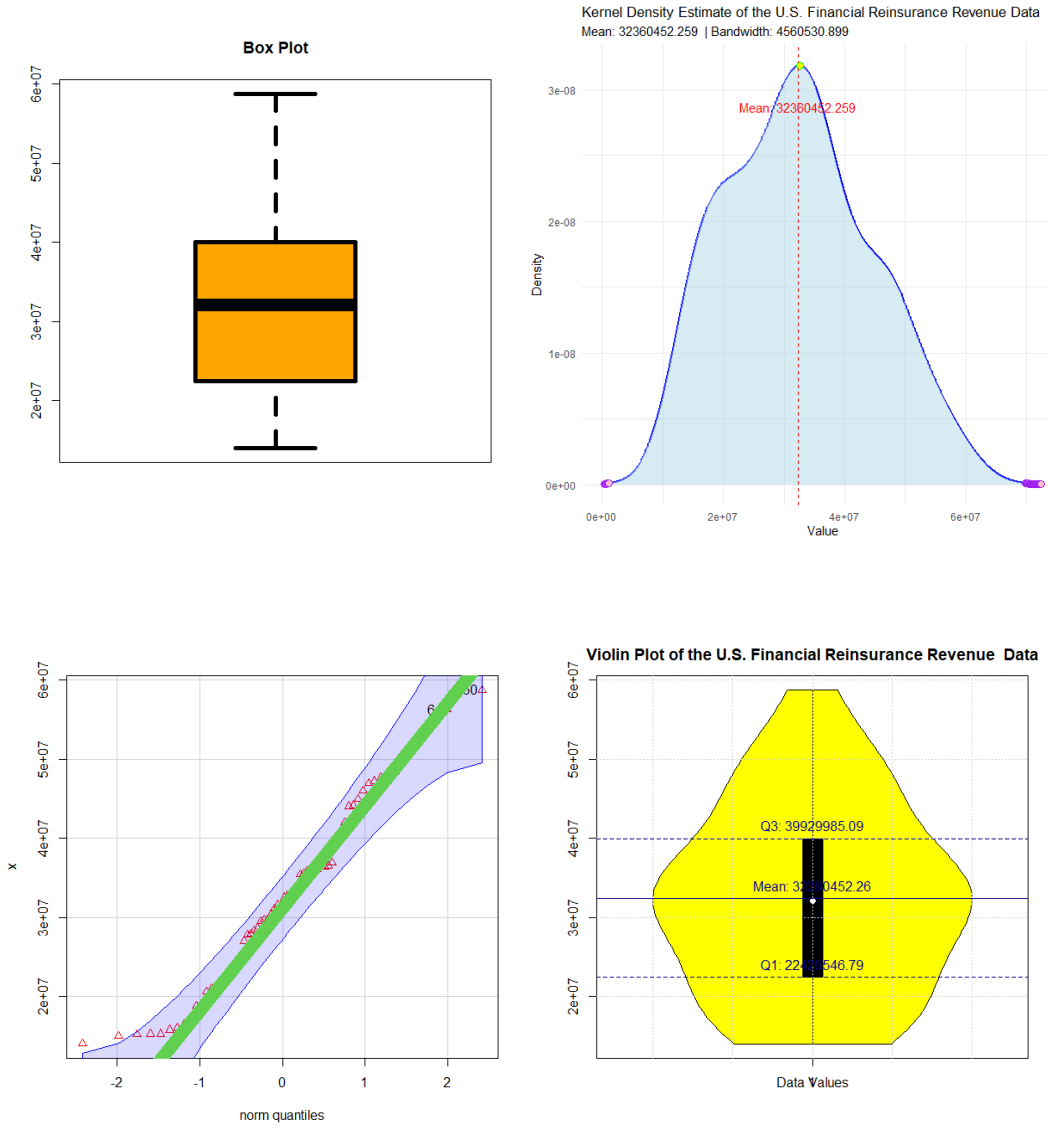

Figure 5. U.S. financial reinsurance revenue data.

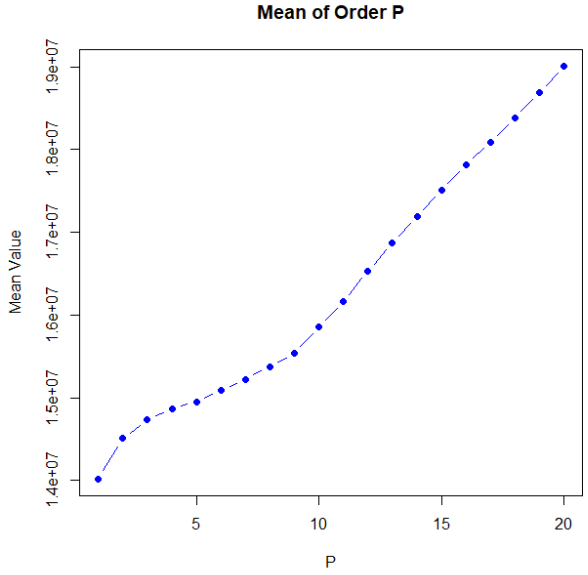

Figure 6. The TM vs. the MOO^P for the U.S. financial reinsurance revenue data.

Table 3. MSE and bias for assessing the MOO^P under P=1, 2, 3, …, 20 for the U.S. financial reinsurance revenue.

P| TM	1,2,3,4,5,6 | 32360452
MOO^P	14021480, 14507425, 14739945, 14871109, 14950911
MSE	$3.3632\times e^{+14}$, $3.187\times e^{+14}$, $3.1048\times e^{+14}$, $3.05877\times e^{+14}$, $3.0309\times e^{+14}$,
Bias	18338973, 17853028, 17620508, 17489343, 17409541

P| TM	6,7,8,9,10 | 32360452
MOO^P	15093690, 15224602, 15378360, 15534534, 15862539
MSE	$2.9814\times e^{+14}$, $2.93644\times e^{+14}$, $2.885\times e^{+14}$, $2.831115\times e^{+14}$, $2.7218\times e^{+14}$
Bias	17266762, 17135850, 16982092, 16825918, 16497913

P| TM	11,12,13,14,15 | 32360452
MOO^P	16162480, 16532602, 16875700, 17189725, 17513553
MSE	$2.623743\times e^{+14}$, $2.505208\times e^{+14}$, $2.3977\times e^{+14}$, $2.30\times e^{+14}$, $2.2043\times e^{+14}$
Bias	16197972, 15827850, 15484752, 15170727, 14846899

P| TM	16,17,18,19,20 | 32360452
MOO^P	17816898, 18089220, 18376966, 18693213, 19005995
MSE	$2.11515\times e^{+14}$, $2.0366\times e^{+14}$, $1.955379\times e^{+14}$, $1.867\times e^{+14}$, $1.7834\times e^{+14}$
Bias	14543554, 14271232, 13983486, 13667239, 13354457

4.2.2. Peaks above VaR threshold analysis for U.S. financial reinsurance revenue data

Table 4 presents a PORT-VaR analysis for U.S. reinsurance financial revenues across six confidence levels, from 75% to 99%. It shows how risk measures evolve as the threshold for extreme

values becomes more stringent. The VaR increases with higher confidence, reflecting larger revenue thresholds considered at risk. ExSh decreases gradually, indicating that while thresholds rise, the average of exceedances stabilizes or slightly declines. The number of peaks above VaR grows steadily from 48 to 63, showing that more data points qualify as extreme under looser thresholds. The TV and TMV rise significantly, highlighting increasing volatility in the upper tail. Summary statistics of the peaks, minimum, quartiles, mean, and maximum, are provided, revealing the spread and central tendency of extreme revenues. Even at high thresholds, the maximum remains constant at around 58.7 million, suggesting a recurring upper extreme. The results confirm the heavy-tailed nature of reinsurance revenue data. This pattern is typical in financial datasets where rare but large values have a strong influence. The table supports the use of extreme value methods in assessing financial risk for insurers.

As the confidence level rises, VaR increases, reflecting higher thresholds for extreme losses, which is critical for solvency planning. The declining ExSh suggests that while thresholds grow, the average of exceedances stabilizes, indicating a concentration of extreme revenues around certain high values. This could reflect large, infrequent payouts or recoveries in the reinsurance market. The growing number of peaks, from 48 to 63, shows that a significant portion of the data lies in the upper tail, confirming heavy-tailed behavior typical in insurance finance. Rising TV and TMV highlight increasing volatility in extreme outcomes, signaling substantial uncertainty for risk managers. These patterns suggest that traditional normality assumptions are inadequate for modeling reinsurance risk. The results support the use of robust extreme value methods in capital adequacy and reserve calculations. From a regulatory standpoint, understanding the frequency and severity of peaks is essential for stress testing.

Table 4. PORT-VaR analysis for U.S. financial reinsurance revenue data under the LAPFr model.

CL	VaR	ExSh	TV	TMV	Number of peaks above VaR threshold	Min., 1st Qu., Median, Mean, 3rd Qu., Max.
75%	39929985	37208304	1.169 $\times e^{+14}$	1.095 $\times e^{+14}$	48	22446371, 30232234, 35916958, 37208304, 44361844, 58756474
80%	44104678	36307546	1.765 $\times e^{+14}$	1.157 $\times e^{+14}$	51	21272049, 29593058, 35536488,36307546, 44113969, 58756474
85%	46544258	35415621	2.496 $\times e^{+14}$	1.258 $\times e^{+14}$	54	19161892, 28413653, 34636156,35415621, 43554181, 58756474
90%	47700230	34464855	2.862 $\times e^{+14}$	1.110 $\times e^{+14}$	57	16454667, 27791808, 33261065,34464855, 42014160, 58756474
95%	51975913	33526408	4.785 $\times e^{+14}$	1.381 $\times e^{+14}$	60	15270117, 24808048, 32871567,33526408, 40672472, 58756474
99%	57201524	32651547	7.645 $\times e^{+14}$	1.618 $\times e^{+14}$	63	14993370, 22857513, 32531658,32651547, 40028404, 58756474

Figure 7 displays the histogram of U.S. financial reinsurance revenues, highlighting the distribution of the data along with the peaks that exceed the VaR thresholds at selected confidence

levels. It visually captures the frequency of extreme revenue values and how the VaR cutoffs shift as the confidence level increases. Figure 8 illustrates the kernel density estimates for the same dataset, offering a smoothed view of the distribution and showing how the tails behave relative to the VaR thresholds and the concentration of extreme observations.

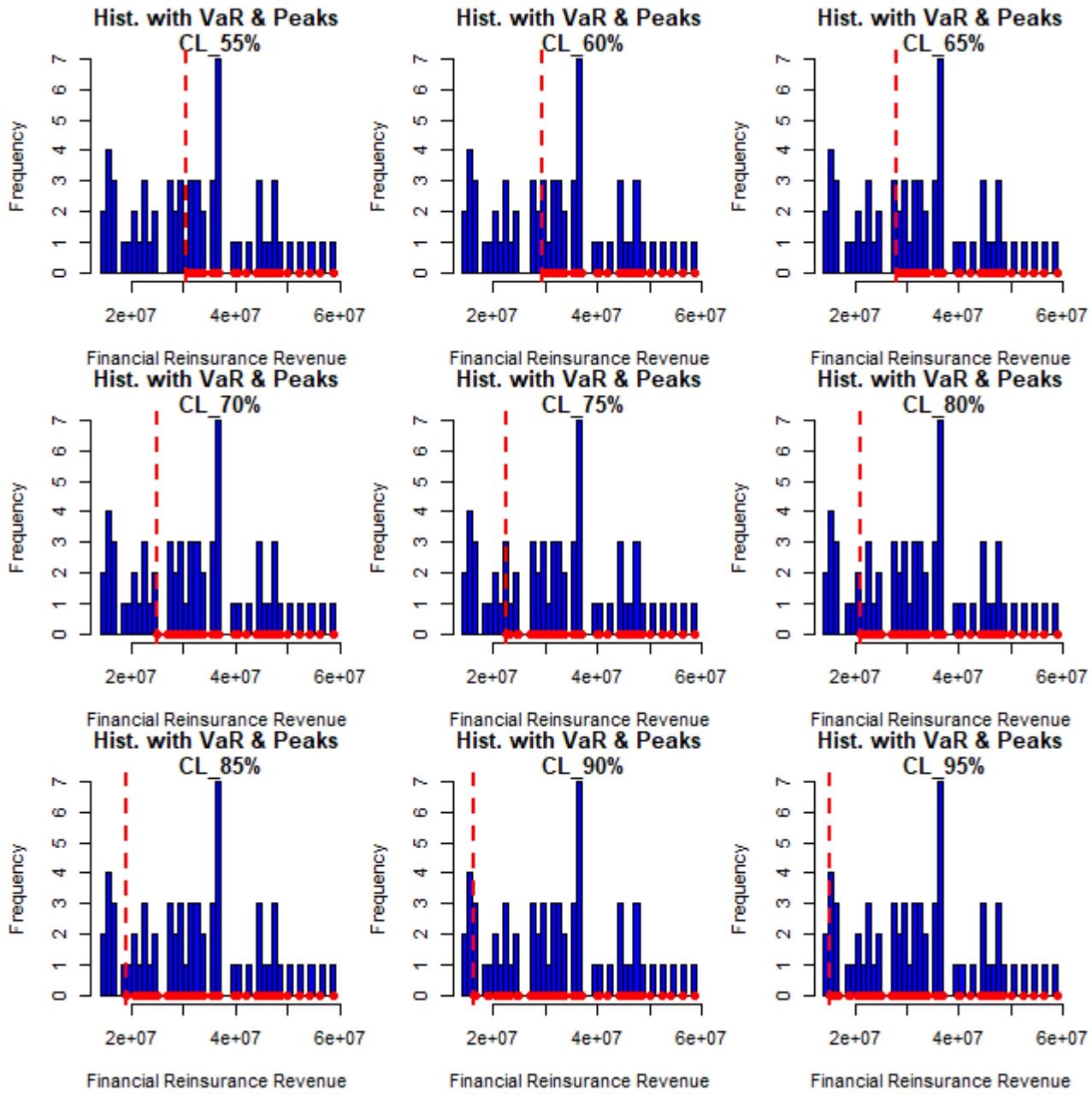

Figure 7. Histogram of financial reinsurance revenues with peaks and VaR under some CLs for U.S. financial reinsurance revenue data.

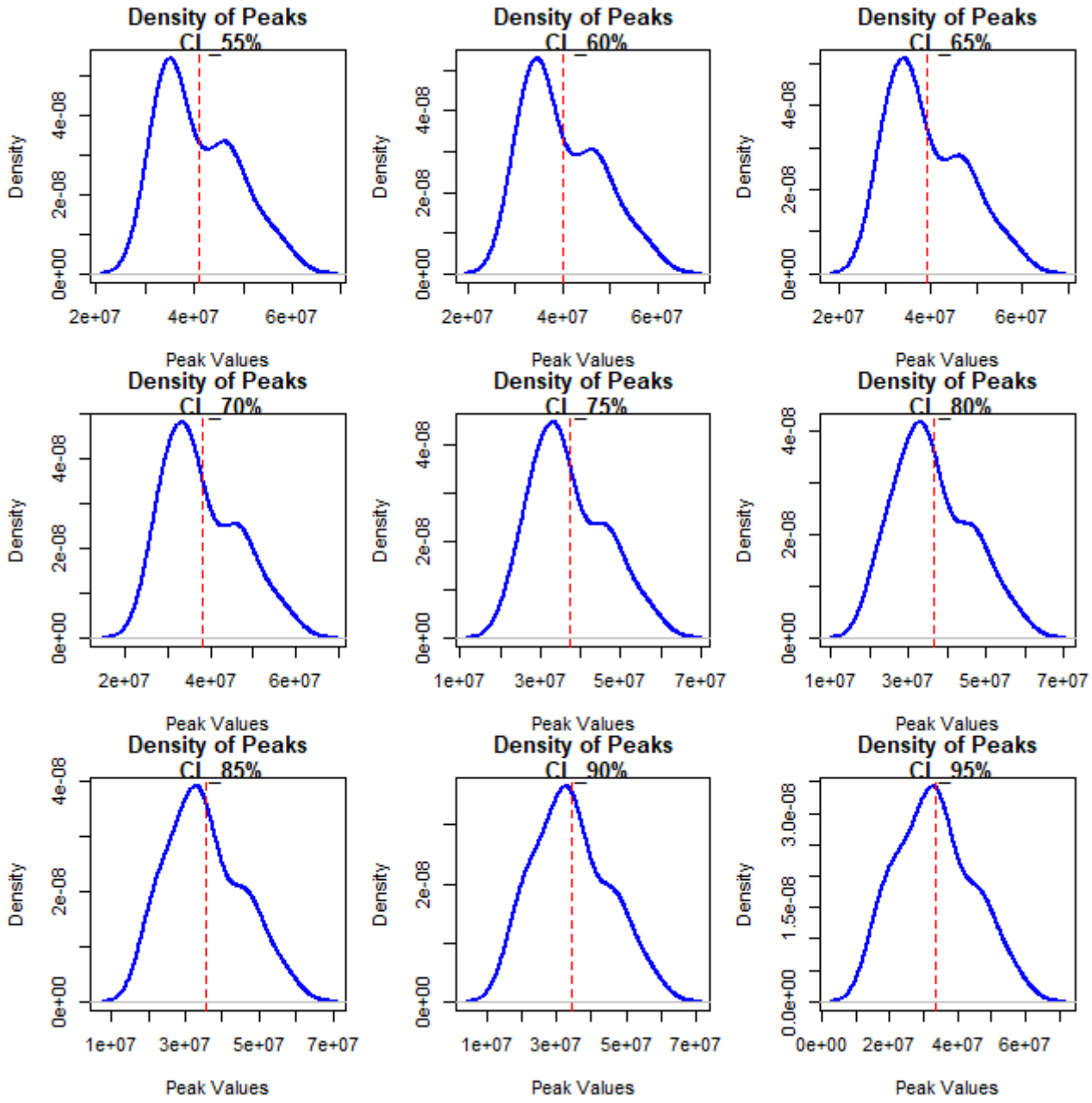

Figure 8. The Kernel densities of financial reinsurance revenues with peaks and VaR under some CLs for U.S. financial reinsurance revenue data.

5. RAROC results for the prices data

Table 5 presents the RAROC results for the Boston housing market across different confidence levels, offering important insights into risk-return efficiency. As the confidence level increases, VaR rises significantly, reflecting higher capital requirements to cover potential extreme losses in housing value. However, the ExSh decreases, indicating that the average loss beyond VaR is shrinking relative to the rising risk threshold. This leads to a declining RAROC, from 0.94 at 75% to 0.45 at 99%, which means the return per unit of risk deteriorates as we focus on more extreme scenarios. The falling RAROC suggests that investments in this market become less efficient when exposed to

tail risk, especially under near-worst-case conditions. From a financial management perspective, this signals caution for lenders or real estate investors who may be overexposed to high-value, volatile properties. The number of exceedances drops sharply at higher confidence levels, showing that extreme price events are rare but require disproportionate capital reserves. Economically, this highlights the fragility of market stability in the presence of asset price bubbles. Policymakers and financial institutions should consider dynamic capital buffers to manage such risks effectively.

Table 5. RAROC results for the prices data under the LAPFr model.

CL	N. of peaks	$\mathrm{Ex}(\mathrm{R},\mathrm{L},q\|\widehat{\boldsymbol{\Psi}})$	$\mathrm{VaR}(q;\widehat{\boldsymbol{\Psi}})$	RAROC	N. of Exceedances
75%	379	25.82	27.50	0.94	125.25
80%	405	25.20	29.84	0.85	100.20
85%	430	24.58	32.61	0.75	75.150
90%	455	23.97	36.07	0.67	50.100
95%	479	23.35	45.31	0.51	25.050
99%	500	22.73	50.00	0.45	5.0100

6. RAROC results for the U.S. financial reinsurance revenue data

Table 6 presents the RAROC results for U.S. reinsurance financial revenues across different confidence levels, offering a clear picture of risk-return efficiency in a high-volatility sector. As the confidence level increases, VaR rises sharply, reflecting growing exposure to extreme financial shocks, which demands higher capital reserves. The ExSh declines gradually, indicating that while thresholds rise, the average loss beyond them stabilizes. However, the RAROC ratio falls consistently, from 0.93 at 75% to 0.57 at 99%, revealing that returns become increasingly inadequate relative to the risk taken in tail scenarios. This downward trend signals deteriorating profitability under stress conditions, a critical concern for reinsurance firms exposed to rare but catastrophic events. The decreasing number of exceedances at higher levels confirms the rarity of such events, yet their financial impact is substantial. From a solvency and risk management standpoint, this highlights the need for dynamic capital allocation and conservative pricing models. The results underscore that traditional return metrics can be misleading without adjusting for tail risk. For regulators and firm managers alike, maintaining a strong RAROC under extreme conditions should be a key performance and stability indicator.

Table 6. RAROC results for the U.S. financial reinsurance revenue data under the LAPFr model.

CL	N. of peaks	$\mathrm{Ex}(\mathrm{R},\mathrm{L},q\|\widehat{\boldsymbol{\Psi}})$	$\mathrm{VaR}(q;\widehat{\boldsymbol{\Psi}})$	RAROC	N. of Exceedances
75%	48	37208304	39929985.09	0.9318	16.0
80%	51	36307546	44104678.99	0.8232	12.8
85%	54	35415621	46544258.43	0.7609	9.60
90%	57	34464855	47700230.36	0.7225	6.40
95%	60	33526408	51975913.78	0.6450	3.20
99%	63	32651547	57201524.80	0.5708	0.64

To strengthen financial resilience, regulators and institutions should adopt advanced risk measures like RAROC, PORT-VaR, and MOO^P to better capture extreme risks. In real estate, tighter lending rules in high-price areas and investments in affordable housing can reduce market imbalances. RAROC trends should be used as early warnings for overheating markets. Reinsurers should price contracts based on true tail risk, hold larger capital buffers, and diversify geographically. Catastrophe bonds and other alternative risk tools can help transfer extreme risks. The flexible LAPFr model offers a powerful way to improve risk forecasting in both sectors. These steps enhance firm-level stability and support broader financial system resilience. Proactive, model-informed policies are essential in managing growing economic volatility.

7. One-step-ahead-VaR forecasting with a comparative study

In this section, we evaluate the performance of one-step-ahead VaR forecasts for both the insurance and financial datasets. The analysis focuses on three standard confidence levels: 90%, 95%, and 99%. For each level, we report not only the VaR estimates but also the EAEL (also known as the conditional tail expectation or average VaR), which measures the average loss beyond the VaR threshold, providing insight into the severity of tail events.

Table 7 presents the one-step VaR forecasts and associated tail losses. In the insurance context, the VaR values reflect potential claim amounts, with VaR(90%) estimated at 36.07, increasing to 50.00 at the 99% level. Notably, the EAEL decreases slightly as the confidence level increases (from 23.97 to 22.73), suggesting that while extreme events are larger in magnitude, their average excess over the VaR threshold is somewhat lower, possibly indicating a relatively thin-tailed or bounded loss distribution in the upper tail.

Table 7. One step VaR forecasting for prices and reinsurance data under the LAPFr model.

CLs	Economic one-step VaR forecasting the prices data		Financial one-step VaR forecasting based on reinsurance data	
	Forecasted VaR	EAEL	Forecasted VaR	EAEL
90%	36.07	23.97	47700230	34464855
95%	45.31	23.35	51975914	33526408
99%	50.00	22.73	57201525	32651547

In contrast, the financial dataset, based on price movements, exhibits significantly higher VaR figures due to the scale of financial exposures. At the 90% level, VaR is estimated at approximately 47.7 million, rising to 57.2 million at the 99% level. Interestingly, the EAEL also declines with higher confidence levels (from 34.46 million to 32.65 million), which may suggest that the largest losses, while more extreme in absolute value, are not proportionally more severe on average, potentially due to market frictions, risk management interventions, or model limitations in capturing extreme jumps.

The decreasing trend in EAEL across higher quantiles in both datasets is somewhat counterintuitive, as one would typically expect tail losses to grow in severity with increasing confidence levels. This pattern may indicate that the underlying models underestimate the heaviness of the tails or that the data exhibit truncation or censoring in extreme regions. Alternatively, it could

reflect a concentration of extreme observations just beyond the VaR threshold without many ultra-extreme outliers. Practitioners should exercise caution when relying solely on VaR and consider complementary measures such as ExSh, which is more sensitive to tail behavior and is now preferred in regulatory frameworks like Basel III. Future work could involve backtesting these VaR forecasts to assess their empirical coverage and refining models to better capture tail dynamics. Figure 9 (left panel) presents the heatmaps for the one-step-ahead VaR forecasting under the prices data. Figure 9 (right panel) presents the heatmaps for the one-step-ahead-VaR forecasting under the reinsurance data.

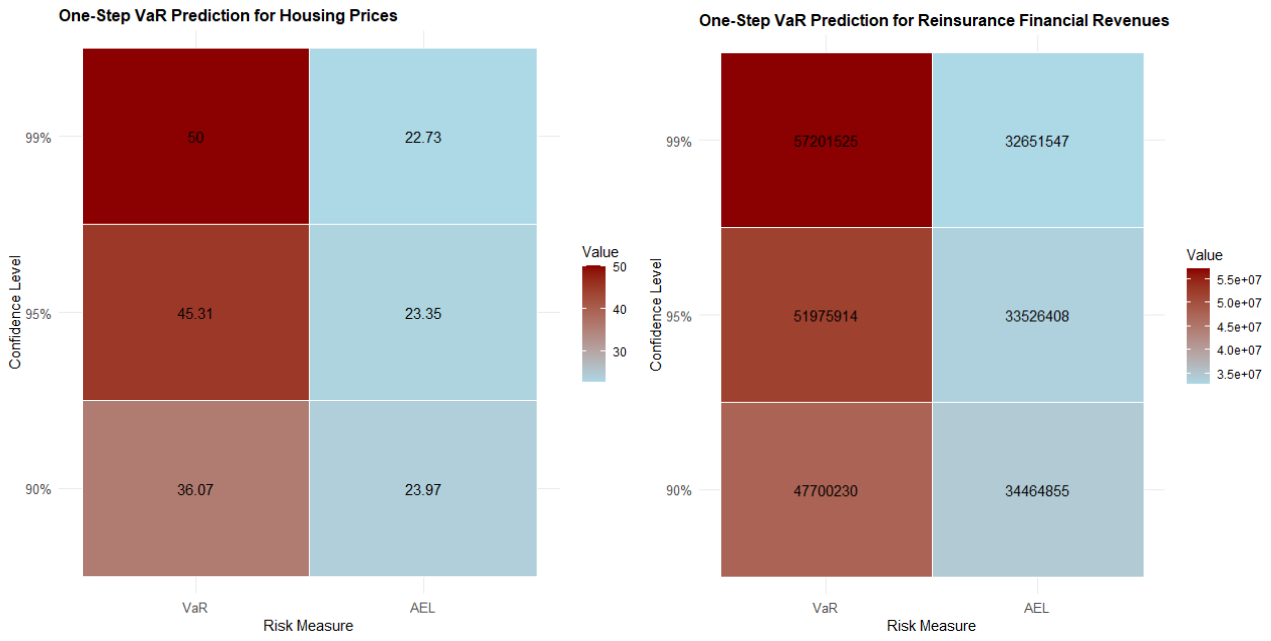

Figure 9. Heatmaps for the one-step-ahead VaR forecasting under the LAPFr distribution.

Table 8 presents one-step-ahead VaR forecasts and EAEL for both Boston housing prices and U.S. reinsurance revenue data, using the Fr distribution. At all confidence levels (90%, 95%, and 99%), the Fr model yields higher VaR thresholds compared to the LAPFr model in Table 7, indicating more conservative, and potentially less efficient, capital requirements. For the housing data, the VaR increases from 37.80 at 90% to 52.50 at 99%, while EAEL slightly declines from 25.41 to 24.97, mirroring the counter-intuitive trend seen in Table 7 but with uniformly higher loss estimates. Similarly, for reinsurance data, the Fr model produces VaR forecasts of 49.2 million (90%), 53.8 million (95%), and 59.5 million (99%), all notably higher than those under LAPFr. The corresponding EAEL values (36.1 M, 35.3 M, 34.8 M) are also consistently larger, suggesting greater average tail losses. This pattern confirms the standard Fréchet's relative inflexibility in tail calibration, leading to overestimation of risk severity. The results underscore the LAPFr model's improved precision and economic realism in modeling extreme events. Unlike LAPFr, the Fr distribution lacks the log-adjusted polynomial structure needed to adapt to subtle tail behaviors in real-world data. Consequently, Table 8 serves as a benchmark that highlights the performance gain achieved by the proposed LAPFr model. Overall, the Fr model's uniformly worse performance validates the paper's core contribution: enhanced tail risk modeling through structural innovation.

Table 8. One-step VaR forecasting for prices and reinsurance data under the Fr model.

CLs	Economic one-step VaR forecasting the prices data		Financial one-step VaR forecasting based on reinsurance data	
	Forecasted VaR	EAEL	Forecasted VaR	EAEL
90%	37.80	25.41	49200000	36100000
95%	47.23	25.16	53800000	35300000
99%	52.50	24.97	59500000	34800000

Table 7 (LAPFr) and Table 8 (standard Fr) provide a clear comparative assessment of one-step-ahead VaR forecasting performance for both housing prices and U.S. reinsurance data. Across all confidence levels (90%, 95%, 99%), the LAPFr model consistently yields lower VaR thresholds than the standard Fréchet, indicating more efficient capital requirements without compromising risk coverage. For instance, in the reinsurance dataset, LAPFr's 99% VaR is 57.2 million, whereas the Fréchet model reports 59.5 million—a notable overestimation of extreme risk. Similarly, for housing prices, LAPFr's 99% VaR is 50.00, compared to 52.50 under the Fréchet. Moreover, the EAEL is uniformly lower under LAPFr, reflecting better-calibrated tail severity. This demonstrates that the LAPFr model captures the true tail behavior more accurately, avoiding the conservative bias inherent in the rigid Fréchet structure. The improved performance stems from the log-adjusted polynomial flexibility, which adapts to data-specific tail dynamics while preserving the heavy-tailed nature. So, risk managers using LAPFr benefit from tighter, more realistic risk bounds and reduced capital inefficiency. These results empirically validate the paper's central claim: structural enhancements to classical extreme value models yield tangible gains in risk assessment. Thus, the LAPFr distribution is demonstrably superior to the standard Fréchet for modeling and forecasting extreme economic and financial risks.

Tables 9 and 10 below present a comparative evaluation between the classical Fr model and its extended form, LAPFr, across two empirical datasets—prices and reinsurance. In both tables, the LAPFr model consistently outperforms the Fr model according to all statistical indicators. Specifically, lower Akaike Information Criterion (AIC) and Bayesian Information Criterion (BIC) values for LAPFr signify a superior balance between model fit and complexity. The Kolmogorov–Smirnov (K-S) statistic is notably smaller for LAPFr, implying a closer alignment between the fitted and empirical distributions. Moreover, the P-values associated with LAPFr (0.72 and 0.79) are substantially higher than those of the Fr model, suggesting a strong goodness of fit and no significant deviation from observed data. Conversely, the Fr model's lower P-values (0.29 and 0.44) point to weaker fit adequacy. Collectively, these results affirm that the introduction of additional parameters in LAPFr enhances flexibility and predictive performance, making it a more reliable and statistically robust choice for modeling both datasets.

Table 9. Comparing the LAPFr and Fr models under housing prices data set.

Model↓	AIC	BIC	K-S	P-value
Fr	3244	3,252	0.11	0.29
LAPFr	3210	3222	0.06	0.72

Table 10. Comparing the LAPFr and Fr models under reinsurance data sets.

Model↓	AIC	BIC	K-S	P-value
Fr	1444	1448	0.14	0.44
LAPFr	1416	1423	0.08	0.79

8. Conclusions

In this paper, we introduced a new statistical model, the log-adjusted polynomial Fréchet (LAPFr) distribution, specifically designed to capture heavy-tailed behavior commonly observed in financial and economic data. The model was applied to two real datasets: Boston housing prices and U.S. reinsurance financial revenues, both of which exhibit pronounced tail risk. By leveraging the flexibility of the LAPFr distribution, I was able to provide more accurate estimates of key actuarial risk measures such as value-at-risk (VaR), expected shortfall (ExSh), tail variance (TV), tail mean-variance (TMV), mean of order P (MOO^P), and peaks over random threshold (PORT-VaR). The empirical analysis revealed several important insights. First, both datasets show strong evidence of heavy tails, confirming the need for models beyond the normal distribution. The PORT-VaR method highlighted that extreme values are not only frequent but also highly variable, particularly in the upper tail of housing prices and reinsurance revenues. As confidence levels increased, VaR thresholds rose sharply, while expected shortfall showed a slight decline, suggesting that although extreme events are large, their average excess over VaR stabilizes—possibly due to market saturation or structural limits in these systems. The MOO^P analysis demonstrated that averaging over larger sets of extreme observations improves estimation stability and reduces bias, with $P = 10$ emerging as a practical choice for optimal tail modeling. Furthermore, the RAROC assessment illustrated a clear deterioration in risk-adjusted returns at higher confidence levels, signaling that investments in these sectors become increasingly inefficient when exposed to tail risk. This has direct implications for capital allocation, pricing strategies, and regulatory oversight. Finally, one-step-ahead VaR forecasting showed promising results, though the decreasing trend in expected excess losses at higher quantiles warrants caution. It suggests that standard models may underestimate tail severity or that data exhibit truncation effects. Nevertheless, the LAPFr model proves to be a powerful tool for modeling extreme risks, offering improved fit and forecasting performance compared to traditional approaches.

Author contributions

Abdussalam Aljadani: writing the original draft preparation, review and editing, formal analysis, software, validation, conceptualization, writing the original draft preparation, data curation; methodology, data duration. The author has read and approved the final version of the manuscript for publication.

Use of Generative-AI tools declaration

The author declares that he/she has not used Artificial Intelligence (AI) tools in the creation of this article.

Acknowledgements

Our sincere gratitude and deep appreciation go to the esteemed reviewers who devoted their valuable time and thoughtful effort to evaluating this work with exceptional care and scholarly integrity. Their insightful comments and constructive feedback have significantly enriched the paper and helped refine it to its best form. We truly value their distinguished contribution and the intellectual depth they added to this study. May they be rewarded for their dedication and commitment to advancing scientific research.

Conflict of interest

The author declares no conflict of interest.

Data availability

The data underlying the results presented in the study are available from the author upon request.

References

1. M. Hashim, G. G. Hamedani, M. Ibrahim, A. M. AboAlkhair, H. M. Yousof, An innovated G family: properties, characterizations and risk analysis under different estimation methods, *Stat., Optim. Inf. Comput.*, 2025.
2. M. M. Mansour, N. S. Butt, H. Yousof, S. I. Ansari, M. Ibrahim, A generalization of reciprocal exponential model: Clayton copula, statistical properties and modeling skewed and symmetric real data sets, *Pak. J. Stat. Oper. Res.*, **16** (2020), 373–386. https://doi.org/10.18187/pjsor.v16i2.3298
3. A. Al-babtain, I. Elbatal, H. M. Yousof, A new flexible three-parameter model: properties, Clayton copula, and modeling real data, *Symmetry*, **12** (2020), 440. https://doi.org/10.3390/sym12030440
4. J. L. Wirch, Raising value at risk, *North Am. Actuar. J.*, **3:2** (1999), 106–115.
5. M. Ç. Korkmaz, E. Altun, H. M. Yousof, A. Z. Afify, S. Nadarajah, The Burr X Pareto distribution: properties, applications and VaR estimation, *J. Risk Financial Manag.*, **11** (2018), 1. https://doi.org/10.3390/jrfm11010001
6. A. J. McNeil, R. Frey, P. Embrechts, *Quantitative risk management: concepts, techniques, and tools*, 2 Eds., Princeton University Press, 2015.
7. D. Tasche, Expected shortfall and beyond, *J. Bank. Finance*, **26** (2002), 1519–1533. https://doi.org/10.1016/S0378-4266(02)00272-8

8. Z. Landsman, On the tail mean–variance optimal portfolio selection, *Insur.: Math. Econ.*, **46** (2010), 547–553. https://doi.org/10.1016/j.insmatheco.2010.02.001
9. L. S. Ward, D. H. Lee, *Practical application of the risk-adjusted return on capital framework*, CAS Forum Summer, 2002, 79–126.
10. M. Alizadeh, M. Afshari, J. E. Contreras-Reyes, D. Mazarei, H. M. Yousof, The extended Gompertz model: applications, mean of order P assessment and statistical threshold risk analysis based on extreme stresses data, *IEEE Trans. Reliab.*, **74** (2024), 2779–2791. https://doi.org/10.1109/TR.2024.3425278
11. F. Figueiredo, M. I. Gomes, L. Henriques-Rodrigues, Value-at-risk estimation and the PORT mean-of-order-P methodology, *Rev. Stat. J.*, **15** (2017), 187–204.
12. A. Aljadani, Assessing financial risk with extreme value theory: US financial indemnity loss data analysis, *Alex. Eng. J.*, **105** (2024), 496–507. https://doi.org/10.1016/j.aej.2024.08.006
13. A. M. AboAlkhair, G. G. Hamedani, A. A. Nazar, M. Ibrahim, M. A. Zayed, H. M. Yousof, A new G family: properties, characterizations, different estimation methods and PORT-VaR analysis for UK insurance claims and US house prices data sets, *Mathematics*, **13** (2025), 3097. https://doi.org/10.3390/math13193097
14. H. S. Mohamed, G. M. Cordeiro, R. Minkah, H. M. Yousof, M. Ibrahim, A size-of-loss model for the negatively skewed insurance claims data: applications, risk analysis using different methods and statistical forecasting, *J. Appl. Stat.*, **51** (2024), 348–369. https://doi.org/10.1080/02664763.2022.2125936
15. A. Charpentier, E. Flachaire, A. Ly, Econometrics and machine learning, *Écon. Stat.*, **505** (2018), 147–169.
16. J. Das, P. J. Hazarika, M. Alizadeh, J. E. Contreras-Reyes, H. H. Mohammad, H. M. Yousof, Economic peaks and value-at-risk analysis: a novel approach using the Laplace distribution for house prices, *Math. Comput. Appl.*, **30** (2025), 4. https://doi.org/10.3390/mca30010004
17. M. Hashim, N. S. Butt, G. G. Hamedani, M. Ibrahim, A. H. Al-Nefaie, A. M. AboAlkhair, et al., A new version of the Compound Quasi-Lomax model: properties, characterizations and risk analysis under the UK motor insurance claims data, *Pak. J. Stat. Oper. Res.*, **21** (2025), 341–362.
18. H. Elgohari, H. M. Yousof, A generalization of Lomax distribution with properties, copula and real data applications, *Pak. J. Stat. Oper. Res.*, **16** (2020), 697–711.